Temporal dynamics of mode instabilities in high-power fiber lasers and amplifiers

Hans-Jürgen Otto,[1,*] Fabian Stutzki,[1] Florian Jansen,[1] Tino Eidam,[1,2] Cesar Jauregui,[1] Jens Limpert,[1,2] and Andreas Tünnermann,[1,2,3]

[1]*Institute of Applied Physics, Abbe Center of Photonics, Friedrich-Schiller-Universität Jena, Albert-Einstein-Str. 15, 07745 Jena, Germany*
[2]*Helmholtz-Institute Jena, Helmholtzweg 4, 07743 Jena, Germany*
[3]*Fraunhofer Institute for Applied Optics and Precision Engineering, Albert-Einstein-Str. 7, 07745 Jena, Germany*
[*]*hans-juergen.otto@uni-jena.de*

Abstract: The temporal behavior of mode instabilities in active large mode area fibers is experimentally investigated in detail. Thus, apart from the onset threshold of mode instabilities, the output beam is characterized using both high-speed camera measurements with 20,000 frames per second and photodiode traces. Based on these measurements, an empiric definition of the power threshold of mode instabilities is introduced. Additionally, it is shown that the temporal dynamics show a transition zone between the stable and the unstable regimes where well-defined periodic temporal fluctuations on ms-timescale can be observed. Finally, it is experimentally shown that the larger the mode-field area, the slower the mode-instability fluctuation is. The observations support the thermal origin of mode instabilities.

OCIS codes: (140.6810) Thermal effects; (140.3510) Lasers, fiber; (140.3425) Laser stabilization; (190.2055) Dynamic gratings.

References and links

1. D. J. Richardson, J. Nilsson, and W. A. Clarkson, "High power fiber lasers: current status and future perspectives," J. Opt. Soc. Am. B **27**(11), B63–B92 (2010).
2. T. Eidam, S. Hanf, E. Seise, T. V. Andersen, T. Gabler, C. Wirth, T. Schreiber, J. Limpert, and A. Tünnermann, "Femtosecond fiber CPA system emitting 830 W average output power," Opt. Lett. **35**(2), 94–96 (2010).
3. J. Limpert, O. Schmidt, J. Rothhardt, F. Röser, T. Schreiber, A. Tünnermann, S. Ermeneux, P. Yvernault, and F. Salin, "Extended single-mode photonic crystal fiber lasers," Opt. Express **14**(7), 2715–2720 (2006).
4. C.-H. Liu, G. Chang, N. Litchinitser, D. Guertin, N. Jacobsen, K. Tankala, and A. Galvanauskas, "Chirally coupled core fibers at 1550-nm and 1064-nm for effectively single-mode core size scaling," CLEO, paper CTuBB3 (2007).
5. T. Eidam, S. Hädrich, F. Jansen, F. Stutzki, J. Rothhardt, H. Carstens, C. Jauregui, J. Limpert, and A. Tünnermann, "Preferential gain photonic-crystal fiber for mode stabilization at high average powers," Opt. Express **19**(9), 8656–8661 (2011).
6. J. Limpert, F. Stutzki, F. Jansen, H-J. Otto, T. Eidam, C. Jauregui, and Andreas Tünnermann, "Yb-doped large-pitch fibres: effective single-mode operation based on higher-order mode delocalization," Light: Science & Applications 1, (2012).
7. T. Eidam, C. Wirth, C. Jauregui, F. Stutzki, F. Jansen, H.-J. Otto, O. Schmidt, T. Schreiber, J. Limpert, and A. Tünnermann, "Experimental observations of the threshold-like onset of mode instabilities in high power fiber amplifiers," Opt. Express **19**(14), 13218–13224 (2011).
8. F. Jansen, F. Stutzki, H. J. Otto, T. Eidam, A. Liem, C. Jauregui, J. Limpert, and A. Tünnermann, "Thermally induced waveguide changes in active fibers," Opt. Express **20**(4), 3997–4008 (2012).
9. C. Jauregui, T. Eidam, J. Limpert, and A. Tünnermann, "The impact of modal interference on the beam quality of high-power fiber amplifiers," Opt. Express **19**(4), 3258–3271 (2011).
10. A. A. Fotiadi, O. L. Antipov, and P. Megret, "Resonantly induced refractive index changes in Yb-Doped fibers: the origin, properties and application for all-fiber coherent beam combining," Frontiers in Guided Wave Optics And Optoelectronics, 209–234 (2010).
11. A. V. Smith and J. J. Smith, "Mode instability in high power fiber amplifiers," Opt. Express **19**(11), 10180–10192 (2011).

#162704 - $15.00 USD Received 8 Feb 2012; revised 26 Mar 2012; accepted 10 May 2012; published 27 Jun 2012

12. C. Jauregui, T. Eidam, H.-J. Otto, F. Stutzki, F. Jansen, J. Limpert, and A. Tünnermann, "Temperature-induced index gratings and their impact on mode instabilities in high-power fiber laser systems," Opt. Express **20**(1), 440–451 (2012).
13. F. Stutzki, H.-J. Otto, F. Jansen, C. Gaida, C. Jauregui, J. Limpert, and A. Tünnermann, "High-speed modal decomposition of mode instabilities in high-power fiber lasers," Opt. Lett. **36**(23), 4572–4574 (2011).
14. M. Laurila, M. M. Jørgensen, K. R. Hansen, T. T. Alkeskjold, J. Broeng, and J. Lægsgaard, "Distributed mode filtering rod fiber amplifier delivering 292W with improved mode stability," Opt. Express **20**(5), 5742–5753 (2012).
15. H. S. Carslaw and J. C. Jaeger, "*Conduction of Heat in Solids*," (Oxford University Press, London, 1948), 191.

1. Introduction

In recent years fiber based laser systems have shown a rapid evolution in terms of output power [1]. Thus, today these systems deliver multi-kW average output powers in continuous-wave operation and they even achieve average powers close to 1 kW when amplifying ultra-short pulses [2]. Simultaneously, fiber lasers and amplifiers typically provide an excellent beam quality due to the guiding properties of fibers. However, with increasing peak powers the detrimental influence of nonlinear effects, e.g. self-phase modulation or stimulated Brillouin- or stimulated Raman-scattering, compromise further scaling of the output power. The most efficient countermeasure to reduce the impact of unwanted nonlinear effects is to increase the mode-field diameter (MFD) of the guided mode and, therefore, to reduce the intensities in the fiber core. However, as a consequence of these enlarged MFDs, the former intrinsic single-mode operation of the fibers cannot be guaranteed any more due to technological limitations in the fabrication process of large mode area (LMA) step-index fibers.

Different approaches have been developed in order to achieve effective single-mode operation even in fibers with large or even very large mode areas [3–6]. However, the average-power scaling of such few-mode designs is limited by a new phenomenon: the sudden onset of mode instabilities that occurs after reaching a certain output-power threshold. Hereby, an initially stable Gaussian-like beam-profile becomes unstable and starts fluctuating rapidly with time. Consequently, the beam quality is reduced [7]. When the pump power is subsequently reduced below the threshold the effect is reversed and the beam-profile becomes stable again.

The power threshold of mode instabilities seems to decrease with increasing MFDs. This way, the power threshold can be beyond 1 kW for fibers with moderate MFDs [2] and it will typically drop noticeably for larger MFDs [8]. Thus, mode instabilities become observable at power levels in the range of some 100 W when using the largest active fibers available. Currently, this effect represents the most limiting factor in average-power scaling of state-of-the-art fiber-laser systems.

A first theoretical explanation for this effect was proposed about a year ago. In this explanation the interference of the fundamental mode (FM) with a low-power higher-order mode (HOMs) causes a periodic intensity pattern in the longitudinal direction [9]. In turn, this beating gives rise to a periodically modified refractive index profile in the fiber-core, either through the resonantly-enhanced nonlinearity [10] or through the thermo-optic effect. This grating has the right period to potentially allow for energy transfer between the interfering modes. However, the exact mechanism ultimately causing this energy transfer and dynamic is still under discussion [11,12]. Nevertheless, a thermally-induced grating is the most plausible explanation for the observed mode instabilities (see chapter 4 and 5).

So far there are only a few systematic experimental studies of mode instabilities. Independent references mention that the fluctuations of the beam-profile are in the range of a few kHz [7,11]. Additionally, the first published videos of mode instabilities provided only limited information about the temporal behavior due to the low sample-rate of the cameras used in the experiments [7]. Therefore, in [13], further insight into the dynamics of mode instabilities has been uncovered by using a high speed camera. These measurements show

#162704 - $15.00 USD Received 8 Feb 2012; revised 26 Mar 2012; accepted 10 May 2012; published 27 Jun 2012

that both the relative phase and relative power content of the involved modes completely redistribute on a millisecond time scale.

To gain further insight into the physics behind mode instabilities, it is important to investigate the temporal dynamics in more detail. In this publication we study the temporal dynamics of different active fibers with high-speed camera and photodiode measurements. The temporal resolution of the videos is in the sub-millisecond range thanks to the camera capturing frames at several kHz. Thus, under-sampling phenomena are avoided. We analyze the temporal dynamics of the beam-profile starting from a stable regime and then going beyond the mode-instability threshold with very strong fluctuations at high average output powers. Additionally, the temporal characteristics of mode instabilities in fibers with different MFDs are analyzed. Finally, the results are discussed in light of the current theoretical understanding.

The manuscript is structured as follows: Section 2 introduces and discusses the high-speed video measurement setup as well as the simplified photodiode measurement. In Section 3 the results of the experimental measurements are shown and the route to mode instabilities is described and discussed. Section 4 expands the investigations to active LMA fibers with different MFD. Finally, in section 5, the results are discussed and the paper ends with a conclusion.

2. High-speed measurements of mode instabilities

Mode instabilities occur in high-power fiber laser systems if a seed-signal is amplified above a certain threshold of average output power. Beyond this threshold, an initially stable Gaussian-like output beam becomes instable (i.e. its shape fluctuates) and the beam quality degrades [7]. However, it is worth mentioning that the output power remains stable in spite of the fluctuating beam. This behavior can be easily observed by means of a camera that records the near-field intensity distribution of the amplified beam. In early experiments conventional cameras were typically used. These devices provide frame-rates of some 10 frames per second (fps), which corresponds to a time resolution in the range of 100 ms. However, as already mentioned in [7,11], mode instabilities occur on a sub-millisecond time-scale. Consequently, a sample rate larger than 10 kHz is required to resolve their temporal behavior. Thus, for the experiments that will be presented in the following, we employed a high-speed camera (pco.dimax). This camera achieves a sample-rate of 20 kHz by recording 576 x 308 pixel images. Any further increase of the sample rate comes at the cost of a reducing the pixel number.

In a first experiment we used the high-speed camera to study the mode instabilities that occur in a ~1.2 m long rod-type large-pitch photonic-crystal fiber (LPF) with a hole-to-hole distance (pitch) of 30 µm (LPF30). In this experiment, the fiber achieved a MFD of 46 µm at its maximum stable output power (~240 W) [8]. As a seed-source we used the oscillator, stretcher and pre-amplifiers of the fiber chirped-pulse-amplification system described in [2]. This oscillator delivers 630 ps pulses at 1040 nm central wavelength with a repetition rate of 39 MHz and an average output power up to 10 W. The fibers under test were placed on an aluminum heat sink over the entire fiber length and they were fixed to it by thermally conductive tape to ensure sufficient cooling.

#162704 - $15.00 USD Received 8 Feb 2012; revised 26 Mar 2012; accepted 10 May 2012; published 27 Jun 2012

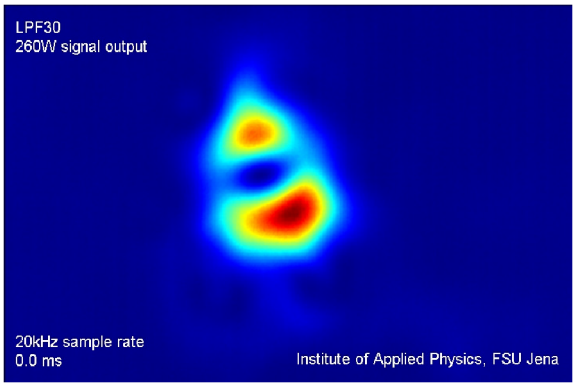

Fig. 1. Single-frame excerpt from a high-speed video recording of mode instability occurring in a rod-type large pitch photonic crystal fiber (LPF) with a hole-to-hole distance of 30 µm (LPF30) (Media 1).

Media 1 (Fig. 1) shows the recorded high-speed video of the near-field beam-profile evolution within a time-period of 40 ms. The output power in this video (260 W) is above the power threshold of this experiment and, therefore, mode instabilities can be observed. The video shows the typical rapid fluctuations caused by the coherent overlap of different fiber modes, namely the fundamental mode (FM) and both orientations of a LP_{11}-like higher-order mode. The intermodal phases and relative power contents change significantly within milliseconds and, therefore, the intensity profile fluctuates [13].

To study the temporal dynamics in more detail we used high-speed videos to derive a simplified method of analysis. This way, we placed an artificial aperture at the center of the intensity distribution seen on the high-speed video and integrate the power within the aperture for each single frame of the video. The thereby obtained time-trace represents the evolution of the relative modal power content. However, the simplified analysis method based on the artificial aperture does not distinguish between modes in contrast to [13]. Therefore, depending on the size and the relative position of the aperture the calculated time traces can be different. Nevertheless, important characteristics of the time traces such as their temporal periodicity or noise are independent of the size and position of the artificial aperture. From an experimental point of view the artificially introduced aperture can be a photodiode which is placed within the laser beam. Therefore, instead of using a high-speed camera a simple photodiode measurement of a portion of the transversal beam profile provides sufficient information on the temporal dynamic. Furthermore, we applied Fourier analysis on the time traces to calculate the corresponding Fourier spectra (FS) to simplify the study on the periodicity of the time traces.

#162704 - $15.00 USD Received 8 Feb 2012; revised 26 Mar 2012; accepted 10 May 2012; published 27 Jun 2012

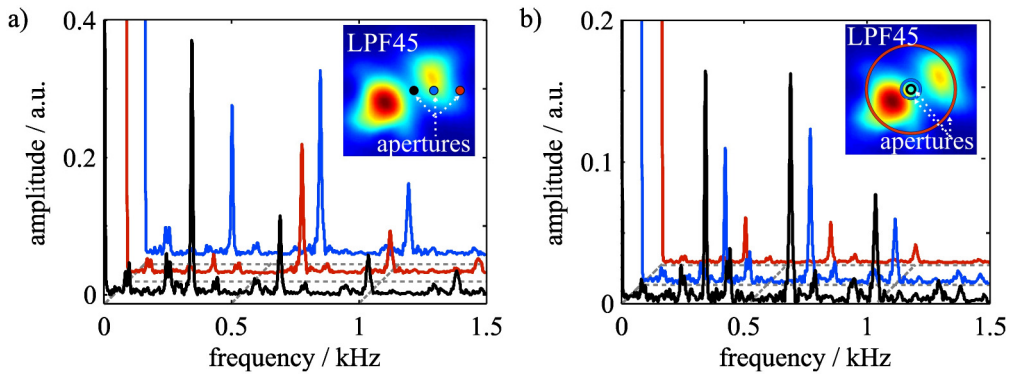

Fig. 2. (a) Fourier spectra of the temporal power evolution within an artificial aperture at three different positions of the beam. The corresponding high-speed video shows mode instabilities in a LPF45 within a time period of 350 ms. The diameter of the apertures is 5% of the MFD corresponding to the incoherent superposition of all high-speed video frames. (b) Fourier spectra corresponding to three centered apertures with three different diameters: 5%, 15% and 40% relative to the MFD.

To exemplify the influence of size and relative position of the aperture on the time traces, the high-speed video of the mode instabilities occurring in a LPF with 45µm pitch (LPF45) is used. In Fig. 2(a) the calculated FS for three different positions of the aperture are shown. Several sharp frequency peaks with different amplitudes can be seen. On the one hand, their center frequency is independent of aperture position and size. The relative amplitudes of these peaks, on the other hand, change depending on the actual position of the aperture. This behavior is due to the fact that the local field amplitudes of the involved modes change across the beam. In any case, all three positions show similar spectral features, albeit with different relative powers. Therefore, placing a photodiode in any part of the beam to measure the power fluctuations suffices to identify the temporal characteristics of the mode instabilities.

Figure 2(b) shows the FS corresponding to three different aperture diameters (5%, 15% and 40% relative to the MFD of the incoherently superposed beam). Unlike in the previous case, here the different diameters cause an approximately homogeneous decrease in amplitude of the spectral features. Since there is no loss of power during mode instabilities (all the power remains confined within the pump core of the fiber), the larger the aperture diameter the more the temporal power variation is averaged out by integration. In the extreme, if the aperture is chosen as large as the pump core, no power fluctuation can be observed. At the same time, however, a very small aperture means low absolute power values, and therefore poor signal to noise ratios.

In consequence, in an experimental setup, both the position and size of the aperture should be chosen in such a way that all peaks are visible and the absolute power is high enough. Typically, if the beam diameter is three to four times the diameter of the photodiode and if it is placed near the center of the beam profile, a good compromise between absolute power value and signal to noise ratio is achieved.

3. The route to mode instabilities

In the literature mode instabilities in high power fiber laser systems have been usually described as a sudden onset of fluctuations happening when reaching a certain output power threshold. Thus, the image that has been transmitted is that below this threshold the beam profile is stable and beyond it mode instabilities occur. But this description is based on low-speed camera and M^2 data. However, these slow characterization methods are not suitable to fully measure mode instabilities due to their long exposure times, slow data acquisition rates or mechanical movements. Consequently, the behavior of fiber laser systems making the transition from stable to unstable could not be characterized in detail in the past.

#162704 - $15.00 USD Received 8 Feb 2012; revised 26 Mar 2012; accepted 10 May 2012; published 27 Jun 2012

For that reason the previously introduced photodiode measurement was used to characterize the output beam while varying the output power. The photodiode was placed near the center of the beam profile and its size was approximately four times smaller than the imaged MFD. Figure 3(a) shows time traces at two different power levels of the commercially available rod-type fiber DC-285/100-PM-Yb-ROD (285/100) that correspond to a beam with (blue trace) and without (red trace) mode instabilities (fiber parameters, see [8]). To ensure their comparability, the time traces have been normalized so that they have the same average value. It can be clearly seen that mode instabilities create strong oscillations in contrast to the stable regime. To quantify the stability of the system the standard deviation normalized to the mean-value (σ_{norm}) of the time traces at different output powers is calculated. A benefit of using σ_{norm} to quantify the stability is its insensitiveness against a variation of the photodiode's position inside the beam profile and the size of the photodiode.

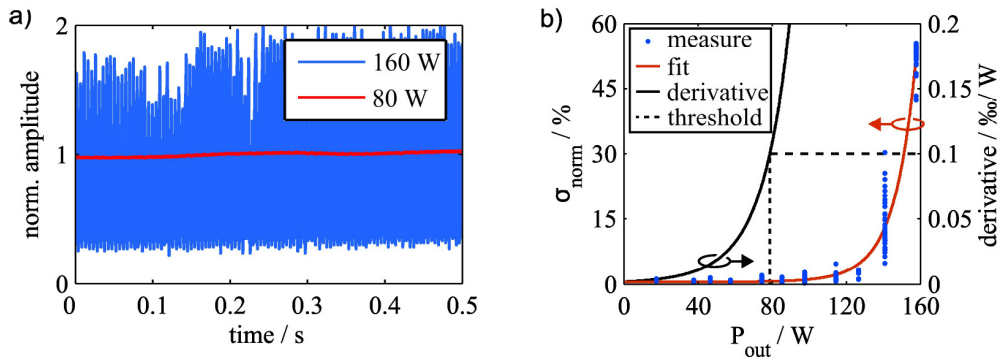

Fig. 3. (a) Two examples of time traces measured by a photodiode following the method described in section 2 at two different power levels. The fiber used is a commercially available DC-285/100-PM-Yb-ROD. The lower power trace (red line) was measured at 80 W and corresponds to the upper limit of the stable operation regime; the high power trace (blue line) was measured at 160 W and corresponds to mode instabilities. Both traces have been normalized to have a mean-value of one. (b) Normalized RMS-deviation σ_{norm} of the time-traces vs. output power. The measured data (blue dots) is fitted by an exponential function (red line) and its first derivative is calculated (black line). The power-value corresponding to a derivative of 0.1 ‰/W is defined as the mode-instability threshold.

The curve so obtained is depicted in Fig. 3(b) and it shows the measured σ_{norm}-values (blue dots). For a specific power level several measurements were done to take into account the spreading of σ_{norm}. It can be seen that with increasing output power the absolute values of σ_{norm} are growing and, simultaneously, the values are more spread around a mean value. This indicates that the beam gets more and more instable at higher power levels and, additionally, that the amplitudes of the oscillations are varying with time.

Comparing Fig. 3(b) with videos recorded by conventional cameras reveal the sensitivity of the σ_{norm} measurement. With a typical camera small beam fluctuations can only be noticed when their amplitude is in the range of several percent of the normalized standard deviation. That corresponds in Fig. 3(b) to an output power of around 140 W. Only for large σ_{norm}-values (several 10%) mode instabilities are clearly observable on such a low-speed camera. However, from Fig. 3(b) it can be seen that the beam gets already slightly instable at lower power-levels. Thus, the photodiode measurement is very well suited to define a stability power threshold.

To characterize the stability of the beam with respect to the output power it is convenient to employ a fit function to average out the spreading of σ_{norm}. In this way, we used the simple exponentially increasing function $y_{fit} = A \cdot exp(B \cdot x) + C$ (red line in Fig. 3(b)) to fit the evolution of σ_{norm}. Based on this fitted curve a power threshold is introduced that represents the maximum average output power of a stable beam profile. For the sake of generalization

#162704 - $15.00 USD Received 8 Feb 2012; revised 26 Mar 2012; accepted 10 May 2012; published 27 Jun 2012

we used the first derivative of the fitted curve to define a threshold to avoid the use of absolute σ_{norm}-values. That provides the benefit of being independent of intrinsic system fluctuations and, therefore, makes the definition more robust and applicable.

The mode instability threshold is reached if the value of the first derivative of the (fitted) evolution of the normalized standard deviation equals 0.1‰/W, i.e.

$$\left.\frac{d\,\sigma_{norm}(P_{out})}{dP_{out}}\right|_{P_{th}} \equiv 0.1\,‰/W \qquad \textbf{(1)}$$

The threshold value of 0.1‰/W is chosen in a strict way to ensure that the so characterized beam is appropriate for further use. From Fig. 3(b) it can be seen that the power threshold is 80 W in the case of the 285/100.

The output power can be further increased with the same linear slope efficiency compared to the stable case even after the onset of mode instabilities. Figure 4(a) shows a wider plot of the evolution of σ_{norm} as a function of output power (up to 350W) for the DC-285/100-PM-Yb-ROD fiber. As illustrated in the graph, the route to mode instabilities typically consists of three regions: a stable region, a transition region and a chaotic region. The system is in the stable region for output powers below the defined mode-instability threshold (region I in Fig. 4(a)). If the output power level is substantially higher than this threshold, the system becomes chaotically unstable (region III in Fig. 4(a). The region in-between corresponds to a transition state (region II in Fig. 4(a).

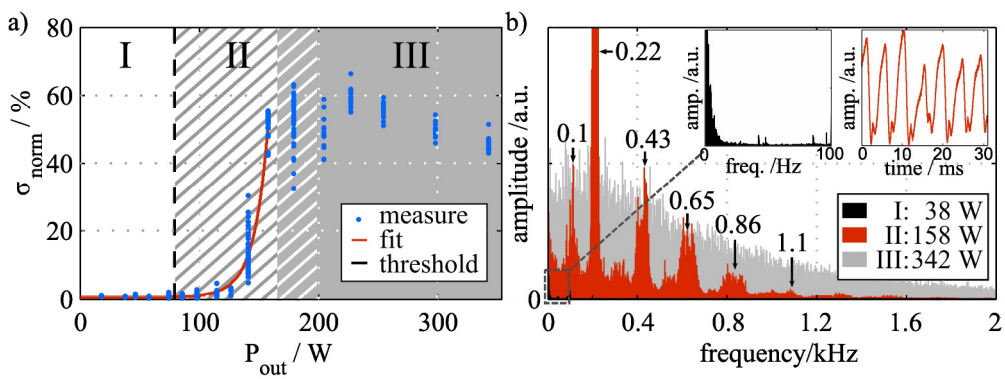

Fig. 4. (a) Evolution of the normalized standard deviation of the photodiode time-traces vs. output power for the DC-285/100-PM-Yb-ROD fiber. There are three distinguishable regions: stable (I), transition (II) and chaotic (III). (b) Characteristic Fourier spectra calculated from the time-traces recorded in the three different regions. The Fourier spectra have been normalized to the same maximum amplitude (the DC peak has the highest amplitude but is not shown).

In order to gain further insight in the dynamic behavior of mode instabilities, we calculated the Fourier spectra of the time traces. Three representative Fourier spectra corresponding to each of the three regions (region I: black spectrum, region II: red spectrum, region III: gray spectrum) are shown in Fig. 4(b). To allow for direct comparison, all the Fourier spectra have been normalized to the same maximum peak amplitude. Looking at Fig. 4(b), it can be stated that the increase of instability is reflected in the Fourier spectra. Thus, it can be seen that with increasing average power more energy is distributed to higher frequency components, i.e. the spectrum broadens. Additionally, the Fourier spectrum of the transition region (red spectrum in Fig. 4(b) and that one of the chaotic region (gray spectrum) are rather different. In the chaotic region the energy is spread over a wide frequency range. In contrast, in the transition region the Fourier spectrum has a large amount of power concentrated in several discrete frequency peaks. It can be seen that most of the peaks are equally spaced.

#162704 - $15.00 USD Received 8 Feb 2012; revised 26 Mar 2012; accepted 10 May 2012; published 27 Jun 2012

Correspondingly, the time traces in the transition region exhibit a periodic sawtooth-like oscillation (see the rightmost inset of Fig. 4(b).

Additionally, the central frequency of the spectral peaks observable in the transition region varies with time. To make this frequency variation visible, a Fourier spectrogram based on the time traces has been calculated and is shown in Fig. 5.

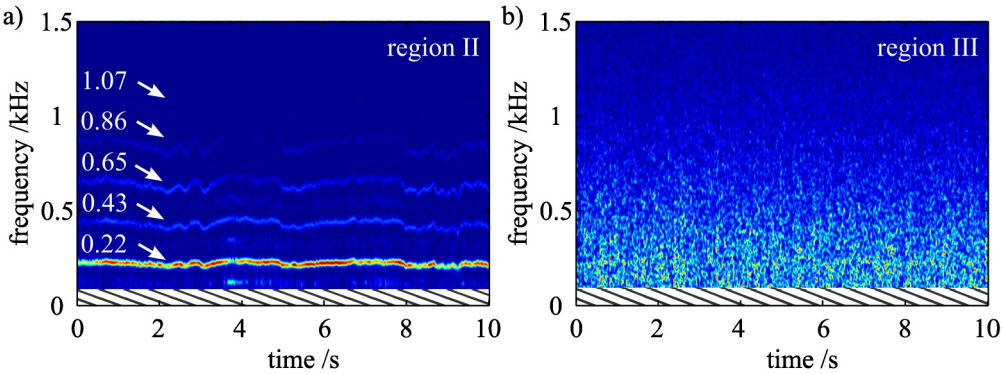

Fig. 5. (a) Spectrogram calculated from a time trace at 158 W of the DC-285/100-PM-Yb-ROD fiber. The frequency and time resolutions are 10 Hz and 10 ms, respectively. The output power corresponds to the transition region (region II) depicted in Fig. 4(a). There are five equally spaced discrete frequency peaks. The frequency separation between the peaks is ~210 Hz. For illustration purposes frequencies below 50 Hz are cut to allow for a proper scaling. (b) Spectrogram calculated from a time trace acquired at 342 W that corresponds to the chaotic region (region III). The energy is spread over a wide frequency range instead of being concentrated around discrete peaks.

The Fourier spectrograms are based on the same time traces that have been used to calculate the Fourier spectra in Fig. 4(b). In the Fourier spectrogram shown in Fig. 5(a) the temporal evolution of the discrete frequencies peaks can be observed. It can be seen that there are temporal fluctuations of the positions of theses peaks, especially around 3 s and 9 s. In these regions the center frequencies of the peaks oscillate. These fluctuations are responsible for the noisy structure of the Fourier spectrum in Fig. 4(b). However, after a certain time these oscillations vanish and the peaks return to their starting frequencies. The origin of these fluctuations is not completely clear yet, but we think that they could be induced by small perturbations of the system (e.g. variations of the pump power/wavelength, cooling cycle).

Such a temporal behavior cannot be observed if the output power lies in the chaotic region. To exemplify this, a Fourier spectrogram corresponding to the chaotic region is illustrated in in Fig. 5(b). In agreement with Fig. 4(b), there are no discrete frequency peaks and the noise-like frequency distribution remains unchanged with time (in spite of any external perturbations that might exist).

4. Comparison of mode instabilities in different fibers

From recent articles [8] it can be inferred that the mode-instability threshold is strongly influenced by the size of the mode field diameter (MFD). As a rule of thumb, it seems that the threshold decreases with increasing MFD. However, the temporal characteristics of mode instabilities have not been studied yet. The analysis methods introduced above, i.e. high-speed camera and photodiode measurements provide the opportunity to quantitatively study and compare the temporal dynamics of mode instabilities of different fibers in detail for the first time. In the following, four fibers with different MFDs are analyzed.

In Table 1 the fibers under test with their corresponding MFDs are listed (for more information about the fibers see [8]). All four fibers had a similar length of around 1 m and were used in a straight configuration without coiling. To ensure comparability, all fibers are used as the main amplifier of the system already introduced in section 2. We characterized the

#162704 - $15.00 USD Received 8 Feb 2012; revised 26 Mar 2012; accepted 10 May 2012; published 27 Jun 2012

power threshold of this system using the LPF30, the LPF45 and the LPF60 as the main amplifier fiber by employing the definition given in (1). In the case of the LPF30 the power threshold was around 300 W, in the case of the LPF45 it was around 200 W, and in the case of the LPF60 it was around 130 W. However, it is worth noting that despite the strict threshold definition, the measured values scatter around the mean value by ± 5% mainly due to the influence of the system stability on mode instabilities (e.g. cooling conditions, stability of the initial mode excitation). Additionally, it has to be noted that the mean power threshold value depends also on the experimental conditions (e.g. seed power, gain characteristics, fiber length, type of cooling). Furthermore, after multiple experiments using the same fiber as the main amplifier a reduction of the power threshold can occur, as reported in [14]. Therefore, the mode instability power threshold is a characteristic value for the whole experimental setup and not for a single fiber.

For the sake of simplicity, the output power of all fibers has been chosen well above the instability threshold of the specific fiber. This means that the high-speed videos of mode instabilities were captured in the chaotic regime. This is done because in this regime mode instabilities are less sensitive to external perturbations as mentioned in the previous section. In the case of the 170/40 the output power was typically around 300 W.

Table 1. Active Fibers Under Test

	DC-170/40-PZ-YB-03 (170/40)	LPF30	LPF45	LPF60
MFD*/µm	29	46	60	75
d_{core} /µm	40	53	81	108
d_{clad} / µm	200	170	255	340
doping area / μm^2	~700	~1400	~3100	~5500
Dop. conc. / ions/m^3	$\sim 3\cdot 10^{25}$	$\sim 3\cdot 10^{25}$	$\sim 3\cdot 10^{25}$	$\sim 3\cdot 10^{25}$

*: The MFD corresponds to the typical maximum stable output power of each fiber.

Media 2 (Fig. 6) shows a high-speed video of the temporal evolution of mode instabilities within a time period of 30 ms for all four fibers. The sample rate of the high-speed camera is 20 kHz and the videos have a native resolution of 576 pixels x 308 pixels. As can be seen from the movie, mode instabilities look similar in terms of the involved modes for the 170/40, the LPF30 and the LPF45. The FM and LP_{11}-like HOMs in both orientations clearly appear during the beam fluctuations in all three fibers. However, mode instabilities in the LPF60 look different. Based on numerical simulations of the fiber and on a subsequent comparison of the overlap with the Ytterbium-doped core area, it can be concluded that in addition to the FM and the LP_{11}-like mode a third mode is involved, namely a LP_{31}-like mode. Hence, in the following we do not carry out any further analysis of this fiber, because it cannot be easily compared with the other fibers.

#162704 - $15.00 USD Received 8 Feb 2012; revised 26 Mar 2012; accepted 10 May 2012; published 27 Jun 2012

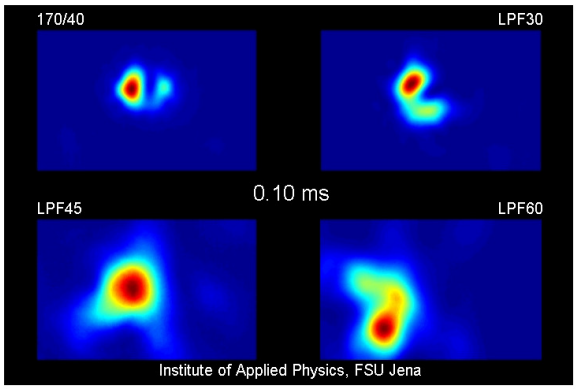

Fig. 6. : Single frame excerpts from a high-speed video recording of mode instabilities occurring in DC-170/40-PZ-YB-03 (170/40), LPF30, LPF45 and LPF60. (Media 2)

Following the procedure detailed in section 2, we retrieve the photodiode-like time traces from each of the high-speed videos. The aperture diameter chosen is 5% of the MFD and it is placed at the center of the beam. The time traces are shown in Fig. 7(a) spanning over a time window of 10 ms. The specific temporal position of the window within the 30 ms long high-speed video is arbitrarily chosen and it represents a typical temporal behavior. The time traces reflect with high fidelity the speed of the beam fluctuations observed in the high-speed videos of the different fibers. Thus, the beam-profile fluctuates fastest for the 170/40 and slowest for the LPF45.

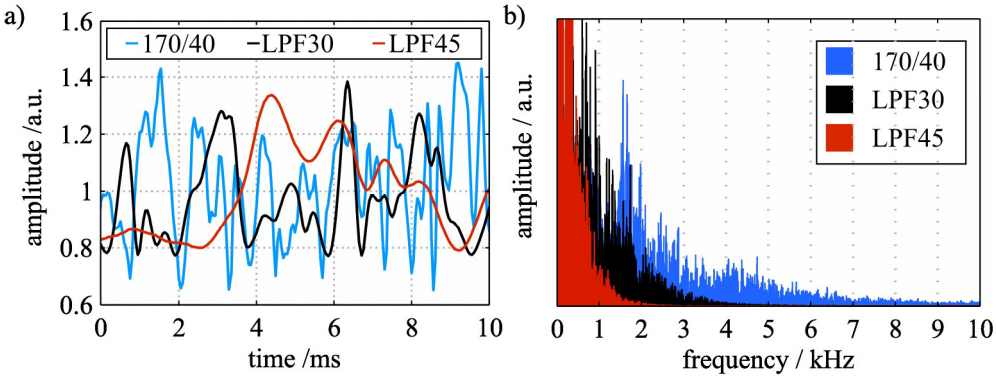

Fig. 7. (a) Retrieved photodiode-like time traces from the high-speed videos of mode instabilities occurring in the 170/40, LPF30 and LPF45 fibers in the chaotic regime over a time period of 10 ms. The time traces are normalized to a mean value of one. (b) Corresponding Fourier spectra normalized to the same maximum amplitude.

The Fourier spectra of the corresponding 30 ms measurement are shown in Fig. 7(b). To allow for direct comparison, the Fourier spectra are normalized again to the same maximum amplitude. From Fig. 7(b) some similarities in the Fourier spectra can be recognized. For example, in all cases the energy is spread over a certain frequency range and it decays with increasing frequency. Moreover, there are no dominant frequency peaks, i.e. all three fibers are in the same chaotic state of mode instabilities. However, there is a significant difference between the spectra: their upper frequency limit. While in the case of the LPF45 most of the energy is distributed in frequencies lower than 2 kHz, the Fourier-spectrum of the LPF30 extends up to 4 kHz and that of the PCF170/40 extends to frequencies higher than 8 kHz.

#162704 - $15.00 USD Received 8 Feb 2012; revised 26 Mar 2012; accepted 10 May 2012; published 27 Jun 2012

5. Discussion

In the previous sections the temporal behavior of different fibers has been experimentally investigated at average powers beyond the mode-instability threshold. Thus, it is interesting to compare the experimental results with the main statements of the possible theoretical explanations.

The first theoretical proposal to explain the origin of mode instabilities was published by Jauregui et al. [9]. They suggested that the refractive index inside the fiber core is modulated by the intensity distribution of two coherently interfering fiber modes via either the resonantly enhanced non-linearity of doped fibers [10] or the thermo-optical effect. Such a periodic modulated refractive index can be understood as a long-period grating with the right period to allow for energy transfer between the interfering modes. Later on, Smith et al. [11] complemented this theory by noting that a phase shift between the interference pattern and the index grating is additionally required to transfer energy between the modes. Thus, the theoretical explanation has been expanded by introducing the notion of a moving grating as the origin for this phase shift and, therefore, for the observed energy transfer. In this proposal the moving grating results from the interference of modes with slightly different wavelengths.

In the high-speed videos of mode instabilities it can be clearly seen that typically three modes are responsible for the beam fluctuations, namely the FM and both orientations of the LP_{11}-like HOM. Moreover, a modal-decomposition method applied to the high-speed videos shows large fluctuations of the relative modal power contents and of their relative phases during beam fluctuations [13]. This observation can be explained by the grating-theory since it provides a mechanism for energy transfer between the modes.

In the third section of this paper we have shown that there is a certain evolution of the stability of the fiber system with increasing output power starting from a stable regime, followed by a transition region and ending in chaos. In the transition regime the system is mainly characterized by a periodic behavior in terms of its temporal evolution. The periodic fluctuations of the beam cause discrete peaks in the Fourier spectrum, which are compatible with a certain movement of the grating, albeit a more complicated one than that suggested in [11]. Additionally, it can be seen from the Fourier spectrograms that possible perturbations influence the system and, therefore, the center position of the discrete peaks can be shifted. After a relaxation period, the system returns to the starting position, namely the starting center frequency. Therefore, it cannot be completely ruled out that these system perturbations play a role in the route to chaos observed in the evolution of mode instabilities with the output power. In this context, as suggested in [12], a grating of growing strength would make the system more and more sensitive to perturbations, until it triggers a chaotic behavior. This point, however, still requires further investigation.

The beam fluctuations that can be observed in the high-speed videos imply that the direction of energy-transfer between the involved modes changes with time. Whether energy is transferred from the FM to the HOM or vice versa is determined by the phase shift between the index grating and the interference pattern. Hence, a change in energy-transfer direction means a change in the sign of the phase shift. This can potentially be caused by a variation in the speed and or direction of propagation of the grating.

It has also been seen that the spectral width of mode instabilities in the chaotic regime (i.e the speed of the beam fluctuations) depends on the MFD. With increasing MFD the amount of power in higher frequencies decreases. A possible explanation for this is a thermal origin of the grating. Thus, the build-up time of the grating would be mostly defined by the transversal thermal-diffusion velocity (TDV) of heat inside the fiber core. Changing the MFD will not influence the TDV but the overall thermal diffusion time (TDT). The larger the core the more time is needed for thermal diffusion. Consequently, if no further mechanisms influence mode instabilities, the shortest time period between two amplitude peaks in the time-traces should be limited by the TDT. In the equivalent picture of Fourier spectra, TDT is

#162704 - $15.00 USD Received 8 Feb 2012; revised 26 Mar 2012; accepted 10 May 2012; published 27 Jun 2012

related to an upper frequency limit. Employing the normalized time in the general temperature distribution formula of a solid rod given in [15],

$$\nu_{\text{lim}} = 4\kappa / \left(C \cdot \rho \cdot MFD^2 \right) \tag{2}$$

where κ is the thermal conductivity with a value for fused silica of κ = 1.38 $W/(m \cdot K)$, ρ is the density of fused silica with a value of 2201 kg/m^3, C is the heat capacity with C = 703 $J/(kg \cdot K)$, the upper frequency limit for the different fibers analyzed in this paper can be roughly estimated. The resulting upper frequency limits are $\nu_{\text{lim}} \approx 4$ kHz for the 170/40, $\nu_{\text{lim}} \approx 2$ kHz for the LPF30 and 1 kHz for the LPF45. The calculated values do not exactly match with the upper frequency limits of the spectra shown in Fig. 7(b), however both the magnitude and the dependency show the expected behavior. This is a strong experimental indication of the thermal origin of mode instabilities.

6. Conclusion

In this work the temporal dynamics of mode instabilities in several state-of-the art active high power fibers with different MFDs have been systematically investigated for the first time. High-speed videos and photodiode time-traces were recorded over a large range of average output powers. The temporal resolution of these measurements was on a sub-ms time scale. Thus, the temporal dynamics of mode instabilities can be completely resolved without suffering from under-sampling phenomena.

In addition to recent publications we showed that there is a transition-region where a formerly stable beam profile gets unstable by increasing the average output-power. A characteristic feature of the transition region is that the temporal fluctuations of the beam-profile occur in a periodic way. This behavior can be identified as discrete frequency peaks in the Fourier spectrum. When the average output power is further increased, the beam-profile gets more and more unstable and fades into a chaotic state. In contrast to the transition region the Fourier spectrum shows a noise-like power distribution.

Based on these observations we proposed a method for the objective definition of the mode-instability power threshold. It employs the derivative of the normalized standard-deviation σ_{norm} of the time traces as a function of the average output power. The power-threshold is reached if the derivative of σ_{norm} equals 0.1‰/W. Please note, however, that the mode instability power threshold characterizes the entire system, i.e. it is not solely determined by the active fiber in use.

The investigations on the dependency of mode instabilities on the MFD showed that with increasing MFD the temporal fluctuations of the beam-profile become slower. Furthermore, the upper frequency limit of the observed mode instabilities agrees reasonably well with an estimation done using the heat diffusion time in the fiber core. This supports the thermal origin of mode instabilities.

Finally, we discussed the experimental results in light of the current theoretical explanation of the effect, i.e. that mode instabilities occur due to a long-period grating induced in the fiber-core by the interference pattern between two modes. It can be shown that the grating offers an explanation for some of the phenomena observed during mode instabilities such as the strong energy transfer between modes. However, there are some aspects that are still waiting for explanation (such as the route to chaos evolution of the mode instabilities). However, this is mainly due to the fact that the dynamic simulation of mode instabilities is still at the very beginning and it is computational challenging. It can be expected that these aspects will also be explained in future articles. Furthermore, some solutions for this effect will certainly arise from the detailed theoretical and experimental understanding of this phenomenon.

#162704 - $15.00 USD Received 8 Feb 2012; revised 26 Mar 2012; accepted 10 May 2012; published 27 Jun 2012

Acknowledgments

The research leading to these results has received funding from the European Research Council under the European Union's Seventh Framework Programme (FP7/2007-2013) / ERC Grant agreement n° [240460] and the Thuringian Ministry of Education, Science and Culture TMBWK) under contract PE203-2-1 (MOFA) and contract B514-10061 (Green Photonics). Additionally, F.J. acknowledges financial support by the Abbe School of Photonics Jena. We would like to thanks the PCO AG, Kelheim, Germany for providing the high speed camera pco.dimax.